DEVELOPMENT OF A MODEL SUPERCONDUCTING HELICAL UNDULATOR FOR THE ILC POSITRON SOURCE*

S.H. Kim[†] and C.L. Doose, ANL, Argonne, IL 60439, U.S.A.

Abstract

The helical undulator for the proposed International Linear Collider (ILC) positron source requires high-permeability steel poles and superconducting coils to meet the ILC parameters. A short-model undulator with a period of 14 mm was designed, fabricated including high-permeability steel poles, and tested in LHe. The ends of the model were designed to wind the Nb_3Sn double helix without any conductor joints. After a few quenches in the first excitation test, the current density in the coil reached 1.28 kA/mm^2, which was approximately 90% of the estimated short-sample critical current density. The periodic on-axis fields were mapped at two azimuth angles. Excluding the end fields, the standard deviation of the field amplitudes and higher harmonic coefficients for the periodic field were less than 7×10^{-3} and 5×10^{-3}, respectively.

INTRODUCTION

The baseline configuration of the proposed International Linear Collider (ILC), which is an electron-positron collider, includes a positron source that relies on a helical undulator as the recommended option. The electron beam with an energy of 150 GeV passes through the undulator, generating gamma rays with an energy of over 10 MeV. The gamma rays are sent through a thin Ti-alloy target to generate the positrons [1,2]. It is envisioned that the ~100-m-long undulator may consist of a number of identical segments, each several meters in length. The ILC design parameters require that the undulator have a magnetic period of about 10 mm, a beam pipe aperture of 5 mm, and an on-axis field of around 1 T. This requires the undulator to have high-permeability steel poles and superconducting (SC) coils with a current density of over 1 kA/mm^2 in the coil.

The first SC helical undulator was constructed by Elias and Madey in 1973 for an early free-electron laser experiment [3]. For the past few years SC, as well as pulsed, helical undulators have been under development for positron sources [4,5]. At Argonne National Laboratory (ANL), model Nb_3Sn SC helical undulators for the ILC are under development. The goal of the program is to develop 10-mm-period models and a field mapping system for the helical undulators.

MAGNETIC FIELD ANALYSIS

The amplitude of the transverse magnetic induction field on the axis of an infinitely long, helical solenoid has

been calculated by Smythe [6]:

$$B_{tr} = \frac{\mu_0 I}{\lambda}\{kr_0 K_0(kr_0) + K_1(kr_0)\}, \tag{1}$$

where p_0 is the permeability in free space, I is the current in the filamentary wire on radius r_0, $k = 2p/\lambda$ with λ as the undulator period along the axis, and K_0 and K_1 are modified Bessel functions.

A helical undulator consists of a double helix carrying an equal current in opposite directions in each helix as illustrated in Fig. 1. When one helix is shifted from the other by a half-period $\lambda/2$ along the z-axis, the usual solenoid axial field is cancelled out, and the amplitude of the transverse field B_0 on the axis, as well as the off-axis field, is enhanced by a factor of two. Kincaid has introduced [7]

$$B_0 = 2B_{tr}, \tag{2}$$

which predicts an on-axis field typically several times higher than if the conductor were given real dimensions instead of being treated as a filament.
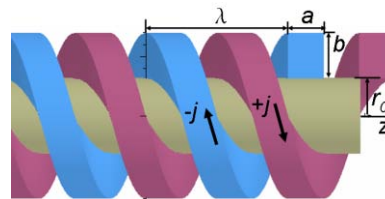

Figure 1: A model helical undulator, with l as the period length, r_0 as the inner radius of the coil, a and b as the coil dimensions, and j as the coil current density. The empty "air space" between the coils may be replaced with high-permeability steel poles.

In cylindrical coordinates (r, f, z) the driving current density J for Fig. 1 may be expressed as the following Fourier series, similar to that for planar undulator analysis [8]:

$$J(kz - \phi) = \sum_{n=1,3,5..}^{\infty} \frac{4j}{n\pi}\sin(nk\frac{a}{2})\cos n(kz - \phi). \tag{3}$$

Then, for $r < r_0$ we calculate the three components of the magnetic field:

$$\mathbf{B} = B_0\{\hat{r}[I_0(kr) + I_2(kr)]\sin(kz - \phi)$$
$$+\hat{\phi}2(-kr)^{-1}I_1(kr)\cos(kz - \phi) + \hat{z}2I_1(kr)\cos(kz - \phi)\}, \tag{4}$$

where I_0 and I_1 are another kind of modified Bessel function and

$$B_0 = \frac{2\mu_0 j\lambda}{\pi} \sin(k\frac{a}{2})\int_{r_0}^{r_0+b} \{krK_0(kr) + K_1(kr)\}\frac{dr}{\lambda}. \quad (5)$$

It should be noted from Eq. (5) that when undulator dimensions are scaled according to a period ratio, the factor $\sin(ka/2)$ and the integrand remain unchanged. Under this condition, the on-axis field B_0 remains unchanged for a constant value of $j\lambda$. Also, the only non-vanishing terms on the axis $r = 0$ in Eq. (4) are the r and ϕ components. Calculations showed that all on-axis fields for $n > 1$ vanished, but not the off-axis fields. This implies that the derived on-axis field has the first harmonic only and the periodic helical field may now be expressed as

$$\mathbf{B}(kz - \phi) = B_0\left\{\hat{r}\cos(kz - \phi) + \hat{\phi}\sin(kz - \phi)\right\}. \quad (6)$$

Harmonics calculations of model undulators with linear and nonlinear steel poles indicated that higher harmonics were less than 2×10^{-3}.

DESIGN AND FABRICATION

Two short-model undulators with an approximate length of 0.25 m were designed with the parameters listed in Table 1. The 10-mm-period model is in the process of fabrication using low-carbon steel poles and stainless steel (SS) beam pipe. The 14-mm model was fabricated first by installing steel poles on the beam pipe. Because of the machining cost and time, "1016 steel," which will have a slightly lower permeability than that of "1010 steel," was used for the poles.

Table 1: Design Parameters for Two Undulator Models

Period (λ)	10 mm	14 mm
Winding bore ($2r_0$)	6.0	7.94
Beam aperture	5.0	6.94
Coil width in the z-direction (a)	3.1	5.0
Coil thickness in the radial (b)	4.1	5.0
Pole width ($\lambda/2 - a$)	1.9	2.0

The ends of the model were designed with SS pins placed radially around a SS disk, with the pins at approximately a 30º angle such that the conductor path would be perpendicular to the pin as shown in Fig. 2. Starting at the terminal end, the conductor was wound tightly against the edge of the core groove helix. At the opposite end, the conductor was wrapped around a pin that allows the conductor to be as close to the disk as possible. The conductor was then return wound on the other helix back to the starting point and wrapped on a pin to start the process again. The next turn on the first helix was wrapped on a pin 180º from the first turn; this required the conductor to be woven in and out of the pins between 0º and 180º. The idea was to alternate the return conductor paths to minimize current loops. After each layer the return pins were advanced by one. There were seven layers and eight pins to distribute the return loops.

This enabled the coil to be wound without any conductor joints. When the directions of the coil winding were reversed at the ends, conductor return paths were carefully chosen to minimize the stray field due to current loops at the ends. There are 39 wires between adjacent poles.

Figure 2: Undulator ends were designed for continuous winding of the double helix without any conductor joints. High-permeability steel poles were installed on the SS beam pipe before the coil winding.

A Nb_3Sn SC wire with a bare diameter of 0.5 mm (approximately 0.63 mm with S-glass insulation) was used for the helix. After pre-heat treatment of the model undulator at 400C for about 50 hrs, the final heat treatment was maintained at 695C for 60 hrs. Figure 3 shows the model with a slightly tinted color after the heat treatment. Before the first electrical test of the undulator in LHe, the brittle Nb_3Sn coil was vacuum impregnated with "Stycast epoxy" (Emerson & Cummings).

Figure 3: The model undulator after the heat treatment.

CALCULATION AND TEST RESULTS

Model Calculations

The amplitude of the on-axis field B_0 and corresponding maximum field in the coil were calculated using Opera-3d and plotted in Fig. 4 [9]. Though the conductor packing factor in the coil was only about 30%, the model calculations assumed a uniform current density in the coil. The permeability data used for the steel poles were for 1010 steel instead of the 1016 steel that was the material actually used for the fabrication. The Nb_3Sn critical current density j_c in the coil was estimated from the j_c at 12 T. The figure shows that the achievable B_0 is about 1 T at $j_c = 1.4$ kA/mm^2.

As indicated in Eq. (5), the on-axis field for the air poles increases as the coil width a is increased. For the

14-mm model with steel poles, when the pole width was reduced to increase the coil width for a range of $a = 3.5 - 5$ mm, B_0 was not increased at all because of the flux saturation in the poles.
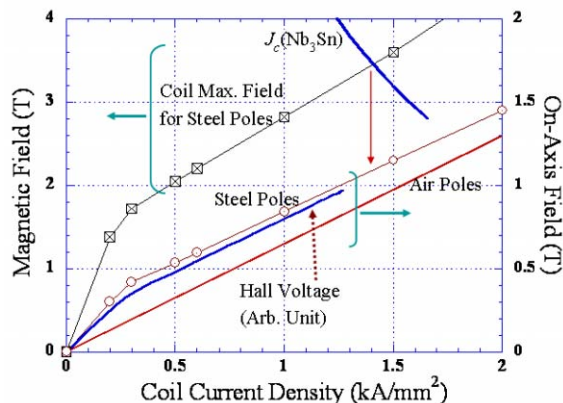

Figure 4: Calculated on-axis field B_0 (*right axis*) and corresponding coil maximum field (*left axis*) for the 14-mm-period model with steel poles are plotted along with the average critical current density (*bottom axis*) for the Nb_3Sn coil at 4.2 K. Also plotted are calculated B_0 for the air-pole model and measured field excitation curve from the Hall probe.

Test Method and Results

The model undulator was supported in a vertical cryostat and cooled in the LHe bath to 4.2 K. The measurement system consisted of a Hall probe at the end of a 1.85-m-long and 6.35-mm-diameter SS rod (slightly smaller than the 6.94-mm aperture of the beam pipe). The rod was coupled to a motorized linear stage along the z-axis and manually operated rotary stage (f-axis). A linear encoder on the z-axis had 1-μm resolution and was used to trigger the measurement of the Hall voltage. Hall probe measurements were performed on-the-fly using a velocity of 2 mm/s and a resolution of 0.1 mm/point. The analog output of the Hall probe instrument was not calibrated. A bellows was installed around the SS rod to minimize changes in temperature of the rod during measurements.

The on-axis fields B_0 measured with the Hall probe are plotted in Fig. 4. The first quench occurred at 675 A (1.05 kA/mm^2). After four more quenches the highest excitation was 820 A (1.28 kA/mm^2). This is approximately 90% of the estimated critical current density of 1.4 kA/mm^2 as indicated by the vertical arrow in Fig. 4. The estimated B_0 at 820 A was around 1 T. The power supply was operated with a voltage limit of 1 V to prevent excess current during quenches. No other protection system was necessary due to the low stored energy of the model.

Field mappings along the z-axis were performed with the Hall probe at two f positions, approximately 90° apart. The periodic on-axis fields measured with an excitation current of 500 A are plotted in Fig. 5. The variations of the end field toward the coil terminal side are shown in the inset. Due to constraints of the mapping setup, the end field for the other end was not measured.
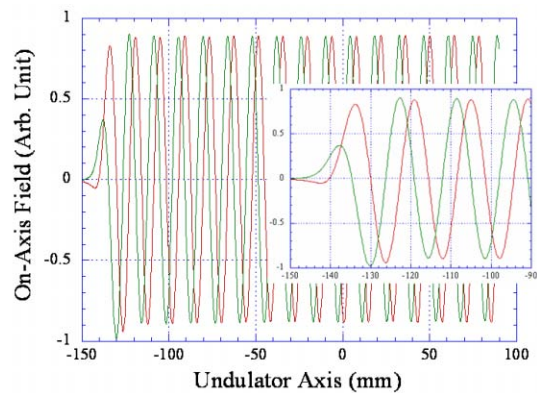

Figure 5: Periodic on-axis fields at two angles 90° apart and (inset) the end fields with an expanded scale.

CONCLUDING REMARKS

The test of the Nb_3Sn model undulator, $\lambda = 14$ mm and $r_0 = 7.94$ mm, achieved B_0 of around 1 T at $j = 1.28$ kA/mm^2 ($0.9j_c$) after a few quenches. The cause of the quenches, which was not investigated, may be due to an imperfect epoxy impregnation. The data of the end field suggests that for the 10-mm-period model, which is under fabrication now, the winding radius for the last two periods may be gradually increased to improve the end field. A preliminary analysis indicated that the standard deviation of the B_0 amplitudes, excluding the end field, was less than 7×10^{-3}. In spite of a relatively large coil/pole width ratio of 2.5, higher harmonic coefficients for the periodic fields up to the 5th harmonic were less than 5×10^{-3}. The latter result is consistent to some degree with the results of the field analysis. The measurement system has not been fully characterized with regard to errors and calibration. These are preliminary results with much work needed to define the limitations of the measurement system.

REFERENCES

[1] http://www.linearcollider.org/cms/.

[2] V. Bharadwaj et al., "Design Issues for the ILC Positron Source," Proc. 2005 PAC, p. 3230, http://www.jacow.org.

[3] L.R. Elias and J.M. Madey, Rev. Sci. Instrum. 50 (1979) 1335.

[4] [5] Y. Ivanyushenkov et al., "Development of a Superconducting Helical Undulator for a Polarized Positron Source," Proc. 2005 PAC, p. 2295, http://www.jacow.org.

[5] A. Mikhailichenko et al., "Pulsed Micro-Undulator for Polarized Positron Production," Proc. 2005 PAC, p. 3676, http://www.jacow.org.

[6] W.R. Smythe, *Static and Dynamic Electricity* (McGraw-Hill, New York, 1939), p. 272.

[7] B.M. Kincaid, J. Appl. Phys. 48 (1977) 2684.

[8] S.H. Kim, Nucl. Instrum. Methods, A 546 (2005) 604.

[9] Opera, Vector Fields Inc., Aurora, IL 60505, USA.